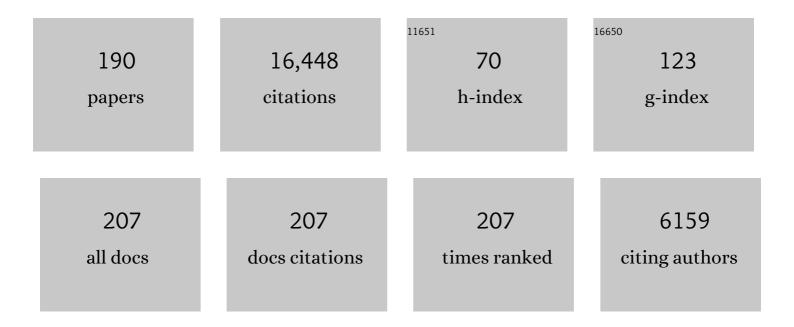
## Joerg Hermann

List of Publications by Year in descending order

Source: https://exaly.com/author-pdf/1609915/publications.pdf Version: 2024-02-01



#	Article	IF	CITATIONS
1	Zircon formation during fluid circulation in eclogites (Monviso, Western Alps): implications for Zr and Hf budget in subduction zones. Geochimica Et Cosmochimica Acta, 2003, 67, 2173-2187.	3.9	570
2	Diffusion of 40Ar in muscovite. Geochimica Et Cosmochimica Acta, 2009, 73, 1039-1051.	3.9	549
3	Aqueous fluids and hydrous melts in high-pressure and ultra-high pressure rocks: Implications for element transfer in subduction zones. Lithos, 2006, 92, 399-417.	1.4	531
4	Experimental zircon/melt and zircon/garnet trace element partitioning and implications for the geochronology of crustal rocks. Chemical Geology, 2007, 241, 38-61.	3.3	481
5	Exhumation as fast as subduction?. Geology, 2001, 29, 3.	4.4	458
6	Sediment Melts at Sub-arc Depths: an Experimental Study. Journal of Petrology, 2008, 49, 717-740.	2.8	419
7	Multiple zircon growth during fast exhumation of diamondiferous, deeply subducted continental crust (Kokchetav Massif, Kazakhstan). Contributions To Mineralogy and Petrology, 2001, 141, 66-82.	3.1	407
8	Accessory phase control on the trace element signature of sediment melts in subduction zones. Chemical Geology, 2009, 265, 512-526.	3.3	364
9	Partial melting of lower crust at 10–15Âkbar: constraints on adakite and TTG formation. Contributions To Mineralogy and Petrology, 2013, 165, 1195-1224.	3.1	358
10	Allanite: thorium and light rare earth element carrier in subducted crust. Chemical Geology, 2002, 192, 289-306.	3.3	323
11	Redistribution of trace elements during prograde metamorphism from lawsonite blueschist to eclogite facies; implications for deep subduction-zone processes. Contributions To Mineralogy and Petrology, 2003, 146, 205-222.	3.1	322
12	Relating zircon and monazite domains to garnet growth zones: age and duration of granulite facies metamorphism in the Val Malenco lower crust. Journal of Metamorphic Geology, 2003, 21, 833-852.	3.4	319
13	Experimental constraints on high pressure melting in subducted crust. Earth and Planetary Science Letters, 2001, 188, 149-168.	4.4	242
14	Experimental study of monazite/melt partitioning with implications for the REE, Th and U geochemistry of crustal rocks. Chemical Geology, 2012, 300-301, 200-220.	3.3	230
15	Temperature and Bulk Composition Control on the Growth of Monazite and Zircon During Low-pressure Anatexis (Mount Stafford, Central Australia). Journal of Petrology, 2006, 47, 1973-1996.	2.8	223
16	Zircon Behaviour in Deeply Subducted Rocks. Elements, 2007, 3, 31-35.	0.5	211
17	The importance of serpentinite mylonites for subduction and exhumation of oceanic crust. Tectonophysics, 2000, 327, 225-238.	2.2	206
18	Geochemistry of continental subduction-zone fluids. Earth, Planets and Space, 2014, 66, 93.	2.5	205

#	Article	IF	CITATIONS
19	Experimental constraints on phase relations in subducted continental crust. Contributions To Mineralogy and Petrology, 2002, 143, 219-235.	3.1	193
20	The robustness of the Zr-in-rutile and Ti-in-zircon thermometers during high-temperature metamorphism (Ivrea-Verbano Zone, northern Italy). Contributions To Mineralogy and Petrology, 2013, 165, 757-779.	3.1	193
21	Fingerprinting the water site in mantle olivine. Geology, 2005, 33, 869.	4.4	191
22	Yo-yo subduction recorded by accessory minerals in the Italian Western Alps. Nature Geoscience, 2011, 4, 338-342.	12.9	178
23	Silicate and carbonate melt inclusions associated with diamonds in deeply subducted carbonate rocks. Earth and Planetary Science Letters, 2006, 241, 104-118.	4.4	176
24	Protracted fluid-induced melting during Barrovian metamorphism in the Central Alps. Contributions To Mineralogy and Petrology, 2009, 158, 703-722.	3.1	176
25	Subduction of water into the mantle: History of an Alpine peridotite. Geology, 1995, 23, 459.	4.4	172
26	Experimental constraints on element mobility from subducted sediments using high-P synthetic fluid/melt inclusions. Chemical Geology, 2007, 239, 228-249.	3.3	171
27	Cooling History and Exhumation of Lower-Crustal Granulite and Upper Mantle (Malenco, Eastern) Tj ETQq1 1 0.7	784314 rg 2.8	BT 10verlock
28	Deep Fluids in Subducted Continental Crust. Elements, 2013, 9, 281-287.	0.5	159
29	Fractionation of Nb and Ta by biotite and phengite: Implications for the "missing Nb paradox― Geology, 2013, 41, 303-306.	4.4	157
30	Geochemical heterogeneity and element mobility in deeply subducted oceanic crust; insights from high-pressure mafic rocks from New Caledonia. Chemical Geology, 2004, 206, 21-42.	3.3	154
31	Tschermak's substitution in antigorite and consequences for phase relations and water liberation in high-grade serpentinites. Lithos, 2013, 178, 186-196.	1.4	153
32	Incompatible element-rich fluids released by antigorite breakdown in deeply subducted mantle. Earth and Planetary Science Letters, 2001, 192, 457-470.	4.4	152
33	The Proterozoic magmatic and metamorphic history of the Banded Gneiss Complex, central Rajasthan, India: LA-ICP-MS U–Pb zircon constraints. Precambrian Research, 2006, 151, 119-142.	2.7	151
34	Quantitative absorbance spectroscopy with unpolarized light: Part II. Experimental evaluation and development of a protocol for quantitative analysis of mineral IR spectra. American Mineralogist, 2008, 93, 765-778.	1.9	150
35	The importance of talc and chlorite "hybrid―rocks for volatile recycling through subduction zones; evidence from the high-pressure subduction mélange of New Caledonia. Contributions To Mineralogy and Petrology, 2008, 155, 181-198.	3.1	148
36	A SHRIMP U–Pb and LA-ICP-MS trace element study of the petrogenesis of garnet–cordierite–orthoamphibole gneisses from the Central Zone of the Limpopo Belt, South Africa. Lithos, 2006, 88, 150-172.	1.4	136

#	Article	IF	CITATIONS
37	Mechanisms of Crustal Anatexis: a Geochemical Study of Partially Melted Metapelitic Enclaves and Host Dacite, SE Spain. Journal of Petrology, 2010, 51, 785-821.	2.8	136
38	An Experimental Study of Carbonated Eclogite at 3{middle dot}5-5{middle dot}5 GPa–Implications for Silicate and Carbonate Metasomatism in the Cratonic Mantle. Journal of Petrology, 2012, 53, 727-759.	2.8	131
39	Constraints on the Proterozoic evolution of the Aravalli–Delhi Orogenic belt (NW India) from monazite geochronology and mineral trace element geochemistry. Lithos, 2010, 120, 511-528.	1.4	129
40	Polyphase inclusions in garnet–orthopyroxenite (Dabie Shan, China) as monitors for metasomatism and fluid-related trace element transfer in subduction zone peridotite. Earth and Planetary Science Letters, 2006, 249, 173-187.	4.4	127
41	39Arâ^'40Ar dating of multiply zoned amphibole generations (Malenco, Italian Alps). Contributions To Mineralogy and Petrology, 2000, 140, 363-381.	3.1	126
42	Experimental evidence for diamond-facies metamorphism in the Dora-Maira massif. Lithos, 2003, 70, 163-182.	1.4	125
43	Melt- versus fluid-induced metasomatism in spinel to garnet wedge peridotites (Ulten Zone, Eastern) Tj ETQq1 1 2006, 151, 372-394.	0.784314 3.1	rgBT /Overlo 125
44	Formation of High-Mg Diorites through Assimilation of Peridotite by Monzodiorite Magma at Crustal Depths. Journal of Petrology, 2010, 51, 1381-1416.	2.8	125
45	Allanite micro-geochronology: A LA-ICP-MS and SHRIMP U–Th–Pb study. Chemical Geology, 2007, 245, 162-182.	3.3	122
46	Composition of fluids during serpentinite breakdown in subduction zones: Evidence for limited boron mobility. Geology, 2004, 32, 865.	4.4	118
47	The infrared signature of water associated with trivalent cations in olivine. Earth and Planetary Science Letters, 2007, 261, 134-142.	4.4	118
48	An experimental investigation of antigorite dehydration in natural silica-enriched serpentinite. Contributions To Mineralogy and Petrology, 2010, 159, 25-42.	3.1	110
49	Ediacaran 2,500-km-long synchronous deep continental subduction in the West Gondwana Orogen. Nature Communications, 2014, 5, 5198.	12.8	109
50	Site-specific hydrogen diffusion rates in forsterite. Earth and Planetary Science Letters, 2014, 392, 100-112.	4.4	108
51	High-pressure veins in eclogite from New Caledonia and their significance for fluid migration in subduction zones. Lithos, 2006, 89, 135-153.	1.4	103
52	Site-specific infrared O-H absorption coefficients for water substitution into olivine. American Mineralogist, 2010, 95, 292-299.	1.9	100
53	Subduction of Continental Crust to Mantle Depth. , 2014, , 309-340.		88
54	Fluid/mineral interaction in UHP garnet peridotite. Lithos, 2009, 107, 38-52.	1.4	87

#	Article	IF	CITATIONS
55	UHP Metamorphism Documented in Ti-chondrodite- and Ti-clinohumite-bearing Serpentinized Ultramafic Rocks from Chinese Southwestern Tianshan. Journal of Petrology, 2015, 56, 1425-1458.	2.8	87
56	Titanium solubility in olivine in the system TiO2–MgO–SiO2: no evidence for an ultra-deep origin of Ti-bearing olivine. Contributions To Mineralogy and Petrology, 2005, 148, 746-760.	3.1	86
57	Quantitative absorbance spectroscopy with unpolarized light: Part I. Physical and mathematical development. American Mineralogist, 2008, 93, 751-764.	1.9	85
58	An Experimental Study of Water in Nominally Anhydrous Minerals in the Upper Mantle near the Water-saturated Solidus. Journal of Petrology, 2012, 53, 2067-2093.	2.8	84
59	Titanium substitution mechanisms in forsterite. Chemical Geology, 2007, 242, 176-186.	3.3	83
60	Fossil crust-to-mantle transition, Val Malenco (Italian Alps). Journal of Geophysical Research, 1997, 102, 20123-20132.	3.3	81
61	Petrology and Geochemistry of the Crust–Mantle Boundary in a Nascent Arc, Massif du Sud Ophiolite, New Caledonia, SW Pacific. Journal of Petrology, 2013, 54, 1759-1792.	2.8	81
62	On the evolution of orogens: Pressure cycles and deformation mode switches. Earth and Planetary Science Letters, 2007, 256, 372-388.	4.4	78
63	Experimentally determined stability of alkali amphibole in metasomatised dunite at sub-arc pressures. Contributions To Mineralogy and Petrology, 2015, 169, 1.	3.1	78
64	Supra-subduction Zone Pyroxenites from San Jorge and Santa Isabel (Solomon Islands). Journal of Petrology, 2006, 47, 1531-1555.	2.8	76
65	Dating prograde fluid pulses during subduction by in situ U–Pb and oxygen isotope analysis. Contributions To Mineralogy and Petrology, 2016, 171, 1.	3.1	75
66	Late Cretaceous-Tertiary tectonics of the southwest Pacific: Insights from U-Pb sensitive, high-resolution ion microprobe (SHRIMP) dating of eclogite facies rocks from New Caledonia. Tectonics, 2005, 24, n/a-n/a.	2.8	74
67	Multistage metasomatism in ultrahigh-pressure mafic rocks from the North Dabie Complex (China). Lithos, 2006, 90, 19-42.	1.4	74
68	Three water sites in upper mantle olivine and the role of titanium in the water weakening mechanism. Journal of Geophysical Research, 2007, 112, .	3.3	74
69	Primary melt inclusions in andalusite from anatectic graphitic metapelites: Implications for the position of the Al2SiO5 triple point. Geology, 2003, 31, 573.	4.4	73
70	Exsolution of thortveitite, yttrialite, and xenotime during low-temperature recrystallization of zircon from New Caledonia, and their significance for trace element incorporation in zircon. American Mineralogist, 2004, 89, 1795-1806.	1.9	73
71	Subducting serpentinites release reduced, not oxidized, aqueous fluids. Scientific Reports, 2019, 9, 19573.	3.3	73
72	Ti site occupancy in zircon. Geochimica Et Cosmochimica Acta, 2011, 75, 905-921.	3.9	72

#	Article	IF	CITATIONS
73	Sub-solidus Oligocene zircon formation in garnet peridotite during fast decompression and fluid infiltration (Duria, Central Alps). Mineralogy and Petrology, 2006, 88, 181-206.	1.1	71
74	Apatite as an indicator of fluid salinity: An experimental study of chlorine and fluorine partitioning in subducted sediments. Geochimica Et Cosmochimica Acta, 2015, 166, 267-297.	3.9	71
75	Submarine backâ€erc lava with arc signature: Fonualei Spreading Center, northeast Lau Basin, Tonga. Journal of Geophysical Research, 2008, 113, .	3.3	70
76	Comparative diffusion coefficients of major and trace elements in olivine at â^1⁄4950 °C from a xenocryst included in dioritic magma. Geology, 2010, 38, 331-334.	4.4	69
77	Arc magmas oxidized by water dissociation and hydrogen incorporation in orthopyroxene. Nature Geoscience, 2019, 12, 667-671.	12.9	69
78	Late Eocene lawsonite-eclogite facies metasomatism of a granulite sliver associated to ophiolites in Alpine Corsica. Lithos, 2011, 125, 620-640.	1.4	66
79	Anorthosite formation by plagioclase flotation in ferrobasalt and implications for the lunar crust. Geochimica Et Cosmochimica Acta, 2011, 75, 4998-5018.	3.9	65
80	Differentiation of Mafic Magma in a Continental Crust-to-Mantle Transition Zone. Journal of Petrology, 2001, 42, 189-206.	2.8	64
81	Lawsonite geochemistry and stability – implication for trace element and water cycles in subduction zones. Journal of Metamorphic Geology, 2014, 32, 455-478.	3.4	64
82	Focused fluid transfer through the mantle above subduction zones. Geology, 2015, 43, 915-918.	4.4	63
83	A Subsolidus Olivine Water Solubility Equation for the Earth's Upper Mantle. Journal of Geophysical Research: Solid Earth, 2017, 122, 9862-9880.	3.4	63
84	Continuous eclogite melting and variable refertilisation in upwelling heterogeneous mantle. Scientific Reports, 2014, 4, 6099.	3.3	61
85	The origin of Eo- and Neo-himalayan granitoids, Eastern Tibet. Journal of Asian Earth Sciences, 2012, 58, 143-157.	2.3	60
86	The role of lower crust and continental upper mantle during formation of non-volcanic passive margins: evidence from the Alps. Geological Society Special Publication, 2001, 187, 267-288.	1.3	58
87	Chlorine and fluorine partitioning between apatite and sediment melt at 2.5 GPa, 800 °C: A new experimentally derived thermodynamic model. American Mineralogist, 2017, 102, 580-594.	1.9	57
88	Identification of growth mechanisms in metamorphic garnet by high-resolution trace element mapping with LA-ICP-TOFMS. Contributions To Mineralogy and Petrology, 2020, 175, 1.	3.1	57
89	Tracing the evolution of calc-alkaline magmas: In-situ Sm–Nd isotope studies of accessory minerals in the Bergell Igneous Complex, Italy. Chemical Geology, 2009, 260, 73-86.	3.3	56
90	Reconstruction of multiple P-T-t stages from retrogressed mafic rocks: Subduction versus collision in the Southern BrasĀlia orogen (SE Brazil). Lithos, 2017, 294-295, 283-303.	1.4	56

#	Article	IF	CITATIONS
91	Polyphase inclusions in the Shuanghe UHP eclogites formed by subsolidus transformation and incipient melting during exhumation of deeply subducted crust. Lithos, 2013, 177, 91-109.	1.4	55
92	Geodynamic cycles of subcontinental lithosphere in the Central Alps and the Arami enigma. Journal of Geodynamics, 2000, 30, 77-92.	1.6	54
93	Dating microstructures by the 40Ar/39Ar step-heating technique: Deformation–pressure–temperature–time history of the Penninic Units of the Western Alps. Lithos, 2009, 113, 801-819.	1.4	54
94	OH-bearing planar defects in olivine produced by the breakdown of Ti-rich humite minerals from Dabie Shan (China). Contributions To Mineralogy and Petrology, 2007, 153, 417-428.	3.1	52
95	Constraints on the thermal evolution of the Adriatic margin during Jurassic continental break-up: U–Pb dating of rutile from the Ivrea–Verbano Zone, Italy. Contributions To Mineralogy and Petrology, 2015, 169, 1.	3.1	50
96	The nature and origin of the Barrovian metamorphism, Scotland: diffusion length scales in garnet and inferred thermal time scales. Journal of the Geological Society, 2011, 168, 115-132.	2.1	49
97	Paleozoic to Triassic ocean opening and closure preserved in Central Iran: Constraints from the geochemistry of meta-igneous rocks of the Anarak area. Lithos, 2013, 172-173, 267-287.	1.4	49
98	Allanite behaviour during incipient melting in the southern Central Alps. Geochimica Et Cosmochimica Acta, 2012, 84, 433-458.	3.9	48
99	Geochemistry of ultrahigh-pressure anatexis: fractionation of elements in the Kokchetav gneisses during melting at diamond-facies conditions. Contributions To Mineralogy and Petrology, 2014, 167, 1.	3.1	48
100	Garnet oxygen analysis by SHRIMP-SI: Matrix corrections and application to high-pressure metasomatic rocks from Alpine Corsica. Chemical Geology, 2014, 374-375, 25-36.	3.3	48
101	The Interplay between Melting, Refertilization and Carbonatite Metasomatism in Off-Cratonic Lithospheric Mantle under Zealandia: an Integrated Major, Trace and Platinum Group Element Study. Journal of Petrology, 2015, 56, 563-604.	2.8	48
102	Age and thermal history of Eo- and Neohimalayan granitoids, eastern Himalaya. Journal of Asian Earth Sciences, 2012, 51, 85-97.	2.3	47
103	Halogens and noble gases in serpentinites and secondary peridotites: Implications for seawater subduction and the origin of mantle neon. Geochimica Et Cosmochimica Acta, 2018, 235, 285-304.	3.9	47
104	Using In Situ Trace-Element Determinations to Monitor Partial-Melting Processes in Metabasites. Journal of Petrology, 2005, 46, 1283-1308.	2.8	45
105	Experimental study of trace element release during ultrahigh-pressure serpentinite dehydration. Earth and Planetary Science Letters, 2014, 391, 296-306.	4.4	45
106	Frozen melt–rock reaction in a peridotite xenolith from sub-arc mantle recorded by diffusion of trace elements and water in olivine. Earth and Planetary Science Letters, 2015, 422, 169-181.	4.4	44
107	Mineral-scale Trace Element and U-Th-Pb Age Constraints on Metamorphism and Melting during the Petermann Orogeny (Central Australia). Journal of Petrology, 2009, 50, 251-287.	2.8	41
108	An experimental investigation of C–O–H fluid-driven carbonation of serpentinites under forearc conditions. Earth and Planetary Science Letters, 2018, 496, 178-188.	4.4	41

#	Article	IF	CITATIONS
109	Deformation mode switches in the Penninic units of the Urtier Valley (Western Alps): Evidence for a dynamic orogen. Journal of Structural Geology, 2008, 30, 194-219.	2.3	39
110	Recrystallization rims in zircon (Valle d'Arbedo, Switzerland): An integrated cathodoluminescence, LA-ICP-MS, SHRIMP, and TEM study. American Mineralogist, 2012, 97, 369-377.	1.9	39
111	Experimental Phase Relations in Altered Oceanic Crust: Implications for Carbon Recycling at Subduction Zones. Journal of Petrology, 2018, 59, 299-320.	2.8	39
112	The role of trace elements in controlling H incorporation in San Carlos olivine. Contributions To Mineralogy and Petrology, 2018, 173, 1.	3.1	39
113	Titanian andradite in a metapyroxenite layer from the Malenco ultramafics (Italy): implications for Ti-mobility and low oxygen fugacity. Contributions To Mineralogy and Petrology, 1994, 116, 156-168.	3.1	38
114	Evidence for multi-stage metasomatism of chlorite-amphibole peridotites (Ulten Zone, Italy): Constraints from trace element compositions of hydrous phases. Lithos, 2007, 99, 85-104.	1.4	37
115	Hafnium isotopes and Zr/Hf of rutile and zircon from lower crustal metapelites (Ivrea–Verbano Zone,) Tj ETQq1 389, 106-118.	1 0.78431 4.4	l4 rgBT /Ove 37
116	The timing of sub-solidus hydrothermal alteration in the Central Zone, Limpopo Belt (South Africa): Constraints from titanite U–Pb geochronology and REE partitioning. Lithos, 2007, 98, 97-117.	1.4	36
117	Contrasting <i>P-T</i> paths within the Barchi-Kol UHP terrain (Kokchetav Complex): Implications for subduction and exhumation of continental crust. American Mineralogist, 2016, 101, 788-807.	1.9	36
118	Evidence for Late Carboniferous subduction-type magmatism in mafic-ultramafic cumulates of the SW Tauern window (Eastern Alps). Contributions To Mineralogy and Petrology, 2002, 142, 449-464.	3.1	35
119	Substitution and diffusion of Cr2+ and Cr3+ in synthetic forsterite and natural olivine at 1200–1500â€`°C and 1†bar. Geochimica Et Cosmochimica Acta, 2018, 220, 407-428.	3.9	35
120	Carbonation of Cl-rich scapolite boudins in Skallen, East Antarctica: evidence for changing fluid condition in the continental crust. Journal of Metamorphic Geology, 2006, 24, 241-261.	3.4	34
121	The influence of oceanic oxidation on serpentinite dehydration during subduction. Earth and Planetary Science Letters, 2018, 499, 173-184.	4.4	34
122	The responses of the four main substitution mechanisms of H in olivine to H2O activity at 1050°C and 3ÂGPa. Progress in Earth and Planetary Science, 2017, 4, .	3.0	33
123	In situ measurement of hafnium isotopes in rutile by LA–MC-ICPMS: Protocol and applications. Chemical Geology, 2011, 281, 72-82.	3.3	32
124	Diffusion of Ti and some Divalent Cations in Olivine as a Function of Temperature, Oxygen Fugacity, Chemical Potentials and Crystal Orientation. Journal of Petrology, 2016, 57, 1983-2010.	2.8	32
125	The effect of fluorine and chlorine on trace element partitioning between apatite and sediment melt at subduction zone conditions. Chemical Geology, 2017, 473, 55-73.	3.3	32
126	Hydrogen diffusion in Ti-doped forsterite and the preservation of metastable point defects. American Mineralogist, 2016, 101, 1571-1583.	1.9	31

8

#	Article	IF	CITATIONS
127	Timescales between mantle metasomatism and kimberlite ascent indicated by diffusion profiles in garnet crystals from peridotite xenoliths. Earth and Planetary Science Letters, 2018, 481, 143-153.	4.4	31
128	Geochronology of accessory allanite and monazite in the Barrovian metamorphic sequence of the Central Alps, Switzerland. Lithos, 2017, 286-287, 502-518.	1.4	30
129	Primary crustal melt compositions: Insights into the controls, mechanisms and timing of generation from kinetics experiments and melt inclusions. Lithos, 2017, 286-287, 454-479.	1.4	29
130	Amphibole and phlogopite in "hybrid―metasomatic bands monitor trace element transfer at the interface between felsic and ultramafic rocks (Eastern Alps, Italy). Lithos, 2010, 117, 135-148.	1.4	28
131	Identification of hydrogen defects linked to boron substitution in synthetic forsterite and natural olivine. American Mineralogist, 2014, 99, 2138-2141.	1.9	28
132	The importance of defining chemical potentials, substitution mechanisms and solubility in trace element diffusion studies: the case of Zr and Hf in olivine. Contributions To Mineralogy and Petrology, 2014, 168, 1.	3.1	28
133	Coupled inter-site reaction and diffusion: Rapid dehydrogenation of silicon vacancies in natural olivine. Geochimica Et Cosmochimica Acta, 2019, 262, 220-242.	3.9	26
134	Episodic formation of Neotethyan ophiolites (Tibetan plateau): Snapshots of abrupt global plate reorganizations during major episodes of supercontinent breakup?. Earth-Science Reviews, 2020, 203, 103144.	9.1	26
135	FTIR spectroscopy of Ti-chondrodite, Ti-clinohumite, and olivine in deeply subducted serpentinites and implications for the deep water cycle. Contributions To Mineralogy and Petrology, 2014, 167, 1.	3.1	25
136	The Molybdenum isotope subduction recycling conundrum: A case study from the Tongan subduction zone, Western Alps and Alpine Corsica. Chemical Geology, 2021, 576, 120231.	3.3	25
137	Mineral solubility and hydrous melting relations in the deep earth: Analysis of some binary A H2O system pressure-temperature-composition topologies. Numerische Mathematik, 2007, 307, 833-855.	1.4	24
138	Generation and Modification of the Mantle Wedge and Lithosphere beneath the West Bismarck Island Arc: Melting, Metasomatism and Thermal History of Peridotite Xenoliths from Ritter Island. Journal of Petrology, 2017, 58, 1475-1510.	2.8	24
139	Experimental constraints on hydrogen diffusion in garnet. Contributions To Mineralogy and Petrology, 2018, 173, 1.	3.1	24
140	In-situ U–Pb dating and Nd isotopic analysis of perovskite from a rodingite blackwall associated with UHP serpentinite from southwestern Tianshan, China. Chemical Geology, 2016, 431, 67-82.	3.3	22
141	Linking tephrochronology and soil characteristics in the Sila and Nebrodi mountains, Italy. Catena, 2017, 158, 266-285.	5.0	22
142	<i>In Situ</i> Oxygen Isotope Determination in Serpentine Minerals by Ion Microprobe: Reference Materials and Applications to Ultrahighâ€Pressure Serpentinites. Geostandards and Geoanalytical Research, 2018, 42, 459-479.	3.1	22
143	The role of the antigorite + brucite to olivine reaction in subducted serpentinites (Zermatt,) Tj ETQq1 1	0.784314 1.2	1 rgBT /Over
144	Experimental subsolidus phase relations in the system CaCO3–CaMg(CO3)2 up to 6.5ÂGPa and implications for subducted marbles. Contributions To Mineralogy and Petrology, 2016, 171, 1.	3.1	20

#	Article	IF	CITATIONS
145	Sustainable densification of the deep crust. Geology, 2020, 48, 673-677.	4.4	20
146	Oxygen isotope analysis of olivine by ion microprobe: Matrix effects and applications to a serpentinised dunite. Chemical Geology, 2018, 499, 126-137.	3.3	19
147	Magmatic flare-up causes crustal thickening at the transition from subduction to continental collision. Communications Earth & Environment, 2021, 2, .	6.8	19
148	Tracing fluid transfers in subduction zones: an integrated thermodynamic and <i>l´</i> <sup>18</sup> O fractionation modelling approach. Solid Earth, 2020, 11, 307-328.	2.8	18
149	Melting of subducted slab dictates trace element recycling in global arcs. Science Advances, 2022, 8, eabh2166.	10.3	18
150	Sensitive high resolution ion microprobe – stable isotope (SHRIMP-SI) analysis of water in silicate glasses and nominally anhydrous reference minerals. Journal of Analytical Atomic Spectrometry, 2015, 30, 1706-1722.	3.0	17
151	Beryllium diffusion in olivine: A new tool to investigate timescales of magmatic processes. Earth and Planetary Science Letters, 2016, 450, 71-82.	4.4	17
152	Hydrogen incorporation and retention in metamorphic olivine during subduction: Implications for the deep water cycle. Geology, 2018, 46, 571-574.	4.4	17
153	Using the elastic properties of zircon-garnet host-inclusion pairs for thermobarometry of the ultrahigh-pressure Dora-Maira whiteschists: problems and perspectives. Contributions To Mineralogy and Petrology, 2021, 176, 1.	3.1	17
154	Melting History of an Ultrahigh-pressure Paragneiss Revealed by Multiphase Solid Inclusions in Garnet, Kokchetav Massif, Kazakhstan. Journal of Petrology, 0, , egw049.	2.8	16
155	Water transfer to the deep mantle through hydrous, Al-rich silicates in subduction zones. Geology, 2021, 49, 911-915.	4.4	16
156	Establishing a protocol for the selection of zircon inclusions in garnet for Raman thermobarometry. American Mineralogist, 2020, 105, 992-1001.	1.9	15
157	Carbon recycled into deep Earth: Evidence from dolomite dissociation in subduction-zone rocks: Comment and Reply. Geology, 2003, 31, e4-e5.	4.4	13
158	Investigation of Fluid-driven Carbonation of a Hydrated, Forearc Mantle Wedge using Serpentinite Cores in High-pressure Experiments. Journal of Petrology, 2020, 61, .	2.8	13
159	Multiple Episodes of Fluid Infiltration Along a Single Metasomatic Channel in Metacarbonates (Mogok) Tj ETQq1 of Geophysical Research: Solid Earth, 2021, 126, .	1 0.784314 3.4	4 rgBT /Over 13
160	Fingerprinting a multistage metamorphic fluid–rock history: Evidence from grain scale Sr, O and C isotopic and trace element variations in high-grade marbles from East Antarctica. Lithos, 2010, 114, 217-228.	1.4	12
161	Evidence for UHP anatexis in the Shuanghe UHP paragneiss from inclusions in clinozoisite, garnet, and zircon. Journal of Metamorphic Geology, 2020, 38, 129-155.	3.4	12
162	Mg diffusion in forsterite from 1250–1600 °C. American Mineralogist, 2020, 105, 525-537.	1.9	12

#	Article	IF	CITATIONS
163	A mapping approach for the investigation of Ti–OH relationships in metamorphic garnet. Contributions To Mineralogy and Petrology, 2020, 175, 1.	3.1	12
164	Changes in the cell parameters of antigorite close to its dehydration reaction at subduction zone conditions. American Mineralogist, 2020, 105, 569-582.	1.9	12
165	Textural and Geochemical Evidence for Magnetite Production upon Antigorite Breakdown During Subduction. Journal of Petrology, 2021, 62, .	2.8	12
166	The oscillatory intergrowth of feldspars in titanian andradite, Little Dromedary, NSW, Australia. European Journal of Mineralogy, 2002, 14, 379-388.	1.3	10
167	Variations of clinopyroxene/melt element partitioning during assimilation of olivine/peridotite by low-Mg diorite magma. Chemical Geology, 2015, 419, 36-54.	3.3	10
168	Let there be water: How hydration/dehydration reactions accompany key Earth and life processes#. American Mineralogist, 2020, 105, 1152-1160.	1.9	10
169	COH-fluid induced metasomatism of peridotites in the forearc mantle. Contributions To Mineralogy and Petrology, 2022, 177, 1.	3.1	10
170	Crustal reworking and hydration: insights from element zoning and oxygen isotopes of garnet in high-pressure rocks (Sesia Zone, Western Alps). Contributions To Mineralogy and Petrology, 2020, 175, 1.	3.1	9
171	Fine-scale phosphorus distribution in coral skeletons: combining X-ray mapping by electronprobe microanalysis and LA-ICP-MS. Coral Reefs, 2011, 30, 813.	2.2	8
172	Phase relations and melting of nominally â€~dry' residual eclogites with variable CaO/Na2O from 3 to 5â€~GPa and 1250 to 1500â€~°C; implications for refertilisation of upwelling heterogeneous mantle. Lithos, 2018, 314-315, 506-519.	1.4	8
173	A combined Fourier transform infrared and Cr K-edge X-ray absorption near-edge structure spectroscopy study of the substitution and diffusion of H in Cr-doped forsterite. European Journal of Mineralogy, 2021, 33, 113-138.	1.3	8
174	Measuring in situ CO2 and H2O in apatite via ATR-FTIR. Contributions To Mineralogy and Petrology, 2021, 176, 1.	3.1	8
175	An Experimental Study of Chlorite Stability in Varied Subduction Zone Lithologies with Implications for Fluid Production, Melting, and Diapirism in Chlorite-Rich Mélange Rocks. Journal of Petrology, 2022, 63, .	2.8	8
176	Pre-metamorphic carbon, oxygen and strontium isotope signature of high-grade marbles from the Lützow-Holm Complex, East Antarctica: apparent age constraints of carbonate deposition. Geological Society Special Publication, 2008, 308, 147-164.	1.3	7
177	Iterative thermodynamic modelling—Part 2: Tracing equilibrium relationships between minerals in metamorphic rocks. Journal of Metamorphic Geology, 2021, 39, 651-674.	3.4	7
178	A shock recovery experiment and its implications for Mercury's surface: The effect of high pressure on porous olivine powder as a regolith analog. Icarus, 2021, 357, 114162.	2.5	5
179	Deep subduction, melting, and fast cooling of metapelites from the Cima Lunga Unit, Central Alps. Journal of Metamorphic Geology, 2022, 40, 121-143.	3.4	5
180	Serpentinite dehydration at low pressures. Swiss Journal of Geosciences, 2022, 115, .	1.2	5

#	Article	IF	CITATIONS
181	How fluid infiltrates dry crustal rocks during progressive eclogitization and shear zone formation: insights from H2O contents in nominally anhydrous minerals. Contributions To Mineralogy and Petrology, 2022, 177, .	3.1	5
182	Reply to comments on "Redistribution of trace elements during prograde metamorphism from lawsonite blueschist to eclogite facies: implications for deep subduction zone processesâ€: Contributions To Mineralogy and Petrology, 2004, 148, 506-509.	3.1	3
183	Crystal structure and phase transition in noelbensonite: a multi-methodological study. Physics and Chemistry of Minerals, 2017, 44, 485-496.	0.8	2

185	Correction to: The role of the antigorite + brucite to olivine reaction in subducted serpentinites (Zermatt, Switzerland). Swiss Journal of Geosciences, 2020, 113, .	1.2	2
186	Hydrogen diffusion in Ti-doped forsterite and the preservation of metastable point defects. American Mineralogist, 2018, , .	1.9	1
187	Relic Oceanic Crust at Subâ€arc Depth: an Example from UHP Eclogites Enclosed in Serpentinites from the Southwestern Tianshan Mountains, China. Acta Geologica Sinica, 2016, 90, 238-238.	1.4	0
188	Acceptance of the Dana Medal of the Mineralogical Society of America for 2018. American Mineralogist, 2019, 104, 624-624.	1.9	0
189	Oxygen diffusion in garnet: experimental calibration and implications for timescales of metamorphic processes and retention of primary O isotopic signatures. American Mineralogist, 2021, , .	1.9	0
190	Depletion and refertilisation of the lithospheric mantle below the Kapsiki plateau (Northern) Tj ETQq0 0 0 rgBT /O	verlock 10 2.0	Tf 50 387 0

Journal of African Earth Sciences, 2022, , 104483.